Silicon Carbide Photomultipliers and Avalanche Photodiode Arrays for Ultraviolet and Solar-blind Light Detection

Alexey Vert, Stanislav Soloviev, Alexander Bolotnikov, and Peter Sandvik
Micro and Nanostructures Technologies
General Electric Global Research Center
Niskayuna, NY, USA
vertiatc@research.ge.com

Abstract— **Silicon carbide is known for its large bandgap and suitability to make highly sensitive ultraviolet photo-detectors. These devices show appreciable quantum efficiencies in the 240 nm – 350 nm wavelength range in combination with low dark currents. We present recent results on 4H-SiC avalanche photodiode arrays and SiC-based solid-state photomultiplier arrays suitable for ultraviolet and solar-blind light detection. A novel SiC-based photomultiplier array was demonstrated. Additional solar-blind optical filter allowed achieving a solar photon rejection ratio of more than 10^6 in combination with 40% quantum efficiency at 280 nm. More than 50% of pixels of the array have demonstrated low dark count rates in the range of several kHz and single photon detection efficiencies of more than 30% at 266 nm in the solar-blind wavelengths range. The photomultiplier array operating in Geiger mode has demonstrated a linearly increasing response with an increase in number of incident photons. We report on the electrical and optical characteristics of solar-blind 4H-SiC avalanche photodiode arrays and photomultipliers.**

I. Introduction

Silicon carbide (SiC) photo detectors are particularly useful for a variety of applications where high temperature and/or high solar photon rejection ratio is required. These applications include but are not limited to corona discharge and flame detection, ultraviolet (UV) astronomy, biological and chemical detection, detection of jet engines and missile plumes. At present photomultiplier tubes (PMTs) and silicon avalanche photodiodes are typically the detectors of choice in these applications, but they require expensive optical filters to achieve a high solar photon rejection ratio as their response extends through the visible and near-UV wavelength ranges [1-2]. Some other applications include down hole gamma sensors and instrumentation where high temperature tolerance and ruggedness are important.

Small-size SiC avalanche photodiodes have been previously demonstrated with a high single photon detection efficiency [3-6] and high solar photon rejection ratio [7]. In this work we present results of the integration of avalanche photodiode arrays and photomultipliers with thin film stack optical filters.

II. Silicon Carbide Avalanche Photodiodes Fabrication

SiC APD arrays, as well as single APD devices, were fabricated using 3-inch diameter n-doped 4H-SiC substrates with surfaces off-oriented 4^o in the [11-20] direction purchased from Cree Research (Durham, NC). The array separate absorption and multiplication (SAM) APD devices had effective p-n junction diameters of 90 μm and areas of UV light exposure of 50 μm in diameter. Single APD test devices diameters varied from 90 to 500 μm. The epitaxial layers structure grown by CVD consisted of a 0.2 μm n^+ cap layer (N_d=2x10^{18} cm^{-3}), a 0.6 μm n^--layer (N_d=2.0x10^{16} cm^{-3}), a 0.15 μm n-layer (N_d=6x10^{17} cm^{-3}), a 0.6 μm n^--layer (N_d=1.4x10^{16} cm^{-3}), and a 2 μm p^+-layer (N_A=10^{18} cm^{-3}) as shown in Fig. 1. The devices were designed as a non-reach-through structure with a low electric field in the n^- absorption layer.

The processing steps used to fabricate the devices included mesa etching, passivation oxide deposition, cathode and anode contact formation, and passivation oxide removal in the active area. Inductively coupled plasma reactive ion etching and photoresist reflow were used to define the mesas with the beveled geometry in order to eliminate edge breakdown effects. A thermally grown SiO_2 film was deposited to passivate the surface. Ni was sputtered to form te n-type contacts and a multiple-layer stack of Ti/Al/Ti/Ni was deposited to form the p-type contacts. Both contacts were annealed simultaneously at 1050^0C in a N_2 ambient. Finally,

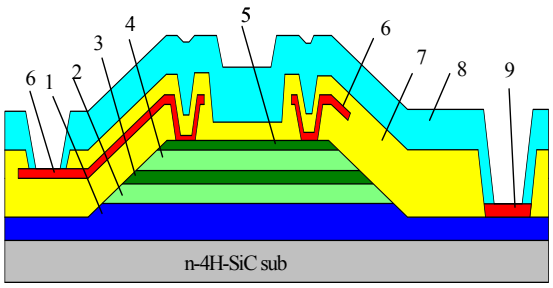

Figure 1. Schematic cross-sectional view of the 4H-SiC SAM-APD , 1 – p-layer, 2 – n- -layer, 3 – n- layer, 4 – n- -layer, 5 – n+-layer, 6 – n-contact, 7 – SiO2 layer, 8 – filter, 9 – p-contact

Ti/Au metal pads were deposited on top of the ohmic contacts and the passivation layer was removed in the active region by wet etching. Fig. 2 shows SEM image of SiC 8x8 APD array.

In order to limit the response of SiC APDs to the solar-blind wavelengths, an optical filter was used to reject the light at wavelengths above 280 nm. A thin film optical filter comprised of HfO_2 and SiO_2 layers was used to provide both a packaged version and a version with the filter deposited directly on the SiC detector. The optical filter deposition was performed by Barr Associates Inc. [8]. Inductively coupled plasma etching was used to open contact windows in the filter after its deposition on APD devices.

III. Silicon Carbide Avalanche Photodiodes Characterization

Fig. 3 shows the responsivity of the fabricated APD devices with and without the filter measured at a reverse bias of 50 V in the linear regime at unity gain. Fig. 4 shows the comparison of the external quantum efficiencies measured on

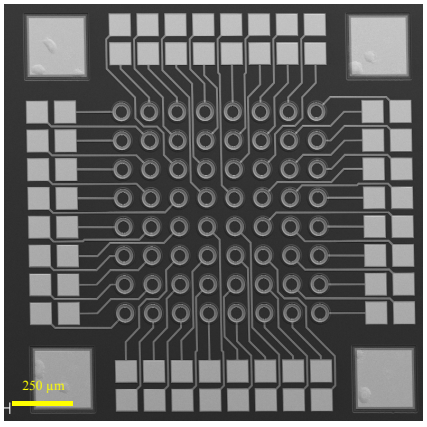

Figure 2. SEM image of SiC 8x8 APD array

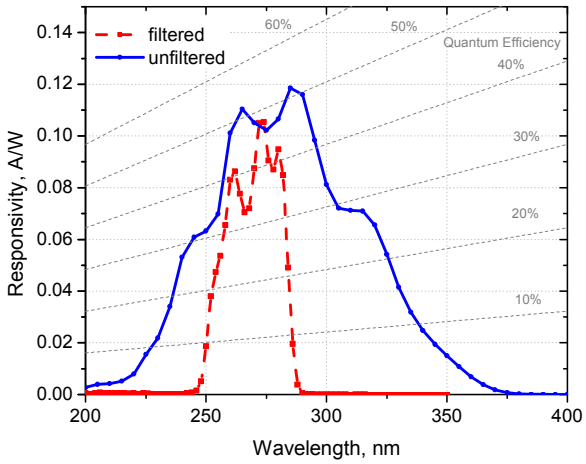

Figure 3. Responsivity and external quantum efficiency of filtered and unfiltered devices.

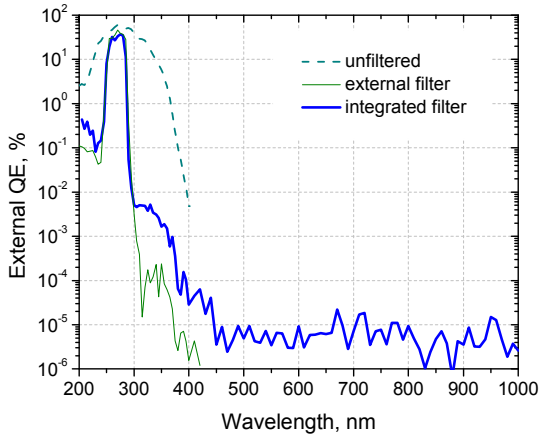

Figure 4. Quantum efficiency measured in a wide range of wavelengths for devices with integrated and external optical filters.

devices with integrated and external optical filters in the wavelengths range from 200 to 1000 nm. Devices with external and integrated solar blind filters showed rejection ratio of at least 10^6 for visible photons, but the rejection ratio of near-UV photons was lower than expected in devices with integrated filter. The limited performance of the devices with an integrated filter may be explained by a high surface roughness of the SiC APD on which the filter was placed. The nature of this roughness may be associated with step bunching (coalescence of several microscopic steps during SiC CVD growth). One can expect to improve the performance of the integrated filter by smoothening the surface of the device before filter deposition.

Although the integrated filter design did not provide a constant 10^6 rejection ratio for the entire solar spectrum, it showed a solution for cost–effective and elegant design of SiC-based solar blind detector suitable for a wide range of applications.

Dark current density curves of a typical SiC APD 8x8 array are shown in Fig. 5. We distinguished three characteristic groups (A, B and C) of the dark current curves. Generally, group A consists of APD devices with the lowest dark currents and very sharp avalanche breakdowns. Group B consists of APD devices with moderate leakage currents and less sharp avalanche breakdowns, while group C consists of APD devices with high leakage currents and soft breakdowns.

Such a variation of leakage currents is partly correlated with the presence of a varying number of dislocations in SiC material local to the measured device [9]. The devices from group A (with the lowest leakage currents) are believed to be defect-free. Fig. 6 shows a typical dark current and gain characteristic measured for a device from this group.

Single photon detection efficiency of separate devices was measured using "quasi-Geiger" method utilizing simple asynchronous passive resistive quenching. The experimental setup schematic is shown in Fig. 7. A 266 nm laser beam focused within the device with an average of 0.3 photons during a 500-ps pulse and an 8,300-Hz repetition rate was used to illuminate the device. The breakdown voltage was measured to be around 193 V and the bias voltage for the "quasi-Geiger" mode measurements was swept between 194 V and 214 V. The SPDE and dark count rate were measured for the same bias to obtain the curve shown in Fig. 8 for devices from three mentioned groups A, B and C.

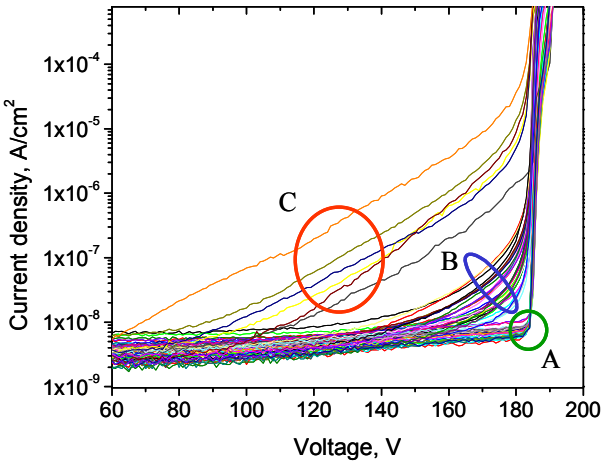

Figure 5. Dark current density curves of a typical SiC APD 8x8 array.

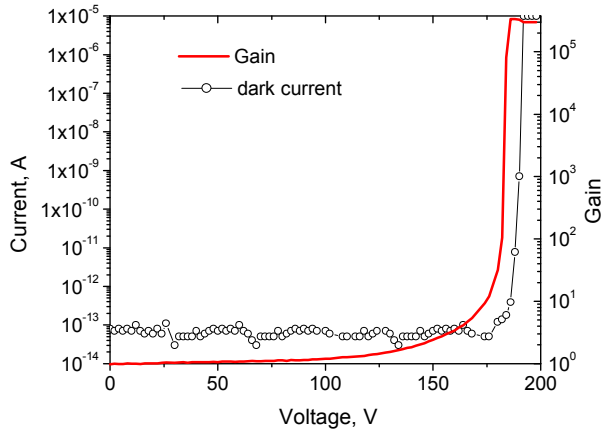

Figure 6. Dark current and gain characteristics of individual SiC APD.

IV. Silicon Carbide Photomultiplier

An 8x8 array of APDs was combined with external quenching resistors to produce a silicon carbide photomultiplier. Forty pixels of the array were selected and connected to the external circuit for photomultiplier measurements. These pixels included only devices from groups A and B. Device pads were connected to the package leads using wire-bonds and the resitor chips were attached directly to the sides of the package in order to minimize parasitics. The readout of the signal was done using a common

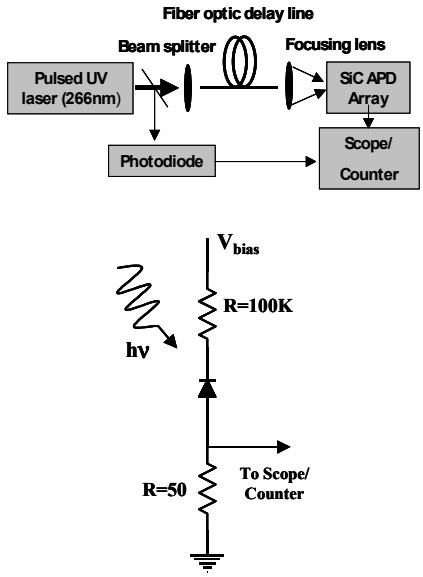

Figure 7. Block diagram and schematics of the photon detection efficiency measurement.

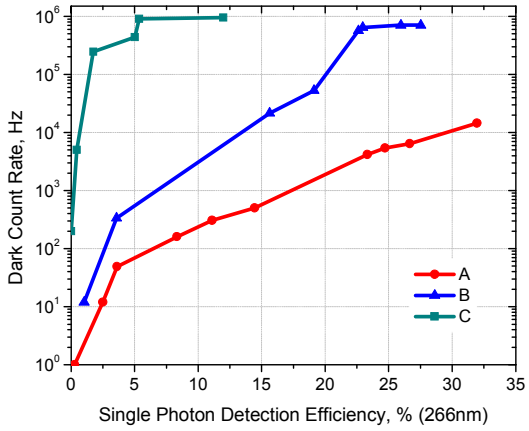

Figure 8. Geiger mode dark count rate versus single photon detection efficiency.

50 Ohm resistor. The photomultiplier did not include the solar blind filter, but it can be integrated on the SiC chip or attached as an external window.

The values of the quenching resistors and the measurement approach were the same as utilized when measuring single photon detection efficiency. A collimated 266-nm laser beam was used to illuminate the array. Fig. 9 shows the dark count rate and the leakage current measured while the bias voltage was swept above the breakdown from 195 V to 210 V. The detection efficiency of a single laser pulse was estimated for "low", "medium" and "high" photon fluxes of 350, 850 and 3300 photons/cm^2 per laser pulse, Fig.10. These photon fluxes corresponded approximately to 0.5, 1.2 and 4 photo-generated holes per laser pulse per total sensitive area of the array.

The photomultiplier array operated in the "low" photon flux regime provides an increased sensitive area and an increased bandwidth, while the "high" photon flux regime provides improved detection efficiency due to the effect of combining avalanche events probabilities of separate pixels.

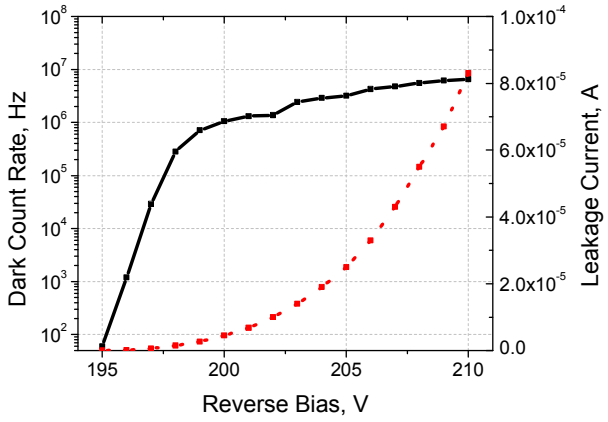

Figure 9. Dark count rate and leakage current of the photomultiplier.

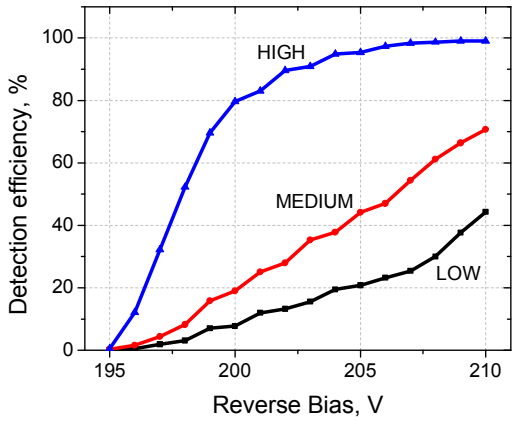

Figure 10. 266-nm laser pulse detection efficiency measured with different photon fluxes – high (3300 photons/cm^2/ pulse), medium (850 photons/cm^2/ pulse) and low (350 photons/cm^2/ pulse).

V. Conclusions

Silicon carbide avalanche photodiode arrays and a novel photomultiplier were fabricated, packaged and tested for ultraviolet light detection. Although the dark count rate of the photomultiplier is significantly higher than the dark count rate of a single defect-free pixel, the advantages of a larger sensitive area, higher bandwidth and higher sensitivity enable novel applications where the detection of faint ultraviolet light pulses is needed. The integrated solar blind filter solution, excellent temperature stability and high single photon detection efficiency of SiC arrays and photomultipliers enable these devices to be adapted in applications including ultraviolet laser ranging and mapping and detection of gamma events from ultraviolet scintillators.

Acknowledgment

The authors wish to thank the late Dr. Henryk Temkin of DARPA for his vision in creating the DUVAP program. We also acknowledge device fabrication and packaging support from Zachary Stum and Brenda Peck. This work was sponsored by US Army under contract W911NF-06-C-0160. Opinions, interpretations, conclusions and recommendations are those of the authors, and not necessarily endorsed by the United States Government.

References

[1] T. Isoshima, et al., "Ultrahigh sensitivity single-photon detector using a Si avalanche photodiode for the measurement of ultraweak biochemiluminescence", Rev. Sci. Instrum., 66, pp. 2922–2926. 1995.

[2] C. Lavigne, A. Roblin, S. Langlois, "Solar-blind UV imaging photon detector with automatic gain control," Measurement Science and Technology, 28, no. 13, pp.713-719, March 2002.

[3] X. Bai, X. Gou, D.C.McIntosh, H.Liu, J.C. Campbell, "High Detection Sensitivity of Ultraviolet 4H-SiC Avalanche Photodiodes", IEEE J. Quantum El., vol. 43, n.12, pp.1159-1162, 2007.

[4] X. Guo, A.L. Beck, Z. Huang, N. Duan, J.C. Campbell, D. Emerson, J.J. Sumarekis, "Performance of Low-Dark-Current 4H-SiC Avalanche Photodiodes With Thin Multiplication Layer", IEEE Trans. Electron Devices, vol. 53, no. 9, pp. 2259-2265, September 2006.

[5] X. Xin, F. Yan, X. Sun, P. Alexandrove, C.M. Stahle, J. Hu, M. Matsumara, X. Li, M. Weiner, and H.J. Zhao, "Demonstration of 4H-SiC UV single photon counting avalanche photodiodes", Electron. Lett., vol. 41, no. 4, pp. 212-214, 2005.

[6] X.Bai, D. Mcintosh, H.Liu, J.Campbell, "Ultraviolet Single Photon Detection With Geiger-Mode 4H-SiC Avalanche Photodiodes", IEEE Phot. Tech. Lett., vol.19, no. 22, pp. 1822-1824, November 2007.

[7] A. Vert, S. Soloviev, P. Sandvik, J. Fronheiser, "Solar blind 4H-SiC single-photon avalanche photodiode operating in Geiger mode", IEEE Phot. Tech. Lett., vol. 20, n. 18, pp. 1587, 2008.

[8] Barr Associates, Inc. Westford, MA 01886 USA.

[9] A.Vert, S. Soloviev, J. Frohneiser, P.Sandvik, "Influence of defects in 4H-SiC avalanche photodiodes on Geiger-mode dark count probability", Mat. Science Forum, vols. 615-617, pp. 877-880, 2009.